Journal of Engineering and Computer Sciences
Qassim University, Vol. 7, No. 2, pp. 135-156 (July 2014/Shaban 1435H)

Improving the Power Conversion Efficiency of the Solar Cells

Abou El-Maaty M. Aly [1,2]

1-Power Electronics and Energy Conversion Department, ERI, NRCB, Egypt

2-College of Computer, Qassim University, P.O.B. 6688, Buryadah 51453, KSA

Tel: +202-3310500, +966-63800050 Fax: +202-3351631, +966-505901562

a_aly@qu.edu.sa & abouelmaaty67@gmail.com

(Received 27/05/2014; Accepted for publication 12/10/2014)

Abstract. In this paper, low-dimensional nanostructures are used to enhance the power conversion efficiency of solar cell (SC). Quantum dots intermediate band (QDIB) is used for this purpose. This idea maintains a large open-circuit voltage and increases the produced photocurrent. The balance efficiency analysis of SC is performed by using the Blackbody spectrum as well as more realistic spectra at AM0 and AM1.5. A comparison between conventional solar cell (CSC), intermediate band solar cell (IBSC), and quantum dots intermediate band solar cell (QDIBSC) is performed. The Schrödinger equation is used to calculate the sub-bandgap energy transition in the quantum dots (QDs) by using the effective mass of charge carriers. Also, the influences of sub-bandgap energy transition, the location of intermediate band (IB), the QDs width size (QDW), and the barrier thickness (BT) between dots are studied on the power conversion efficiency of SC. The results show that the efficiency of SC is significantly improved when it is based on nanostructures.

***Keywords*:** Quantum dots, Intermediate Band, Efficiency, Solar Cell, Intermediate Band Solar Cell

1. Introduction

In the past decades, the whole world commenced to feel the severity of the deficiency in the fossil fuel. Therefore a large number of researchers around the world began to look for and study the alternative energy to compensate conventional energy loss. The solar energy is one of the important topics for alternative energy and improving this technology can clearly reduce the problem of energy in the world [1 - 3]. Therefore many researchers at Nanopower Research Laboratories focus on the enhancement of SC power conversion efficiency by using nanostructures with suitable adjusted properties [4 - 6]. The new proposed concepts are called third-generation solar cell such as hot carrier cells, tandem cells, and intermediate-band cells [2, 5, 7 - 10]. The intermediate energy bands are established within a forbidden gap of a bulk semiconductor material when a superlattice low-dimensional nanostructure (quantum well, wire, dots) of other semiconductor material injected within a bulk semiconductor material [11 - 13]. This structure is called heterostructure and it allows for the proper operation of the IBSC. For quantum well and wire heterostructures, the photogenerated charge carriers will lose energy through thermalization due to the high density of states available in the in-plane and longitudinal direction respectively [14]. Also, the Fermi level will not be split into the number of bands but it will be split into two levels similar to the CSC. Therefore the lowest intermediate band will act as the conduction band (CB) and the heterostructure will behave like the CSC [15, 16]. For QDs heterostructure, it will provide zero density of states between the excited bands due to the discrete energy spectrum therefore the thermalization is reduced. Each band is thermally isolated therefore the Fermi energy level will be split into the number of bands and charge concentration in each band is described by its own chemical potential as required for improving IBSC operation [14, 17]. Figure (1a) shows the QDIBSC with the barrier material surrounding the QDs. Where the QDs are made of the materials such as Ge, InAs, InAsN…..etc. which have smaller bandgap energy than the barrier materials such as Si, GaAs, GaAsN….etc. The superlattice structure is an array of closely spaced QDs therefore a sufficient amount of wavevectors overlapped to form the intermediate energy bands [6, 10], Fig. (1b). These bands are very important in the advanced solar cell because they allow the absorption of low energy photons addition to the normal absorbed photons processes, and the efficiency is improved via increasing the generated photocurrent [18]. In this paper, the theoretical study for CSC, IBSC, and QDIBSC will be discussed and the balance efficiency is studied versus structural and different locations of intermediate-band in IBSC to optimize the efficiency. The organization of this paper includes the related work in section 2. The balanced efficiency analysis in section 3, the conventional solar cell and one intermediate band solar cells (one-IBSCs) are studied in sections 4 and 5. The quantum dots one intermediate band solar cell (one-QDIBSC) with ternary materials structure and different QDs width sizes and barrier thickness is discussed in section 6. Finally, a conclusion of the results and future works are summarized in section 7.

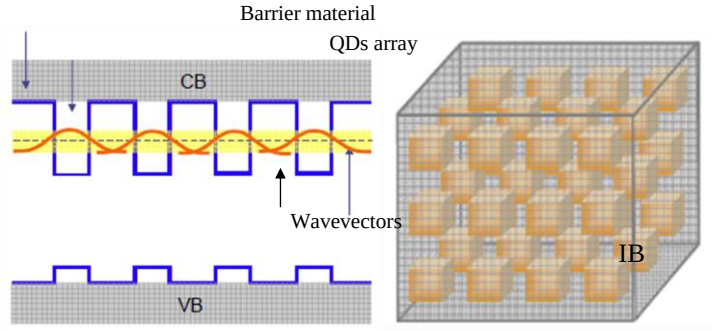

Fig. (1). (a) Diagram of the QDs inside a barrier semiconductor material. (b) Intermediate energy bands of an array of QDs

2. Related Work

Conventional solar cells have demonstrated the ability to achieve power conversion efficiency values near the maximum theoretical limit, i.e., Shockley–Queisser limit of 31% - 41% [19, 20]. However, the maximum power conversion limitation for CSCs is lower than desired, due to energy loss for solar photons with energy exceeding the bandgap energy and absence of SC response to solar photons with energy below the bandgap energy. Power conversion efficiency has been improved for tandem and multi-junction solar cells (54.93% for 1 sun and 67.23% for 1000 suns), but these devices are more complex and are accompanied by higher manufacturing costs [21]. In recent years, IBSC have been proposed to exceed efficiency limitations of CSCs [19, 22]. Previous calculations have suggested a theoretical 63.2% efficiency limitation [22] for one-IBSCs, motivating experimental efforts to realize these promising solar cell devices. Several approaches have been proposed to practically realize an IBSC, including quantum dots [23 - 27], impurity-band SCs [28], and dilute semiconductor alloys [29, 30]. The present work will concentrate on the theoretical study and comparison of CSC and IBSC to improve the power conversion efficiency. Thereafter, alloys for the bulk and injected semiconductor materials will be selected to achieve the concept of IBSC by using quantum dots with varying the size and the distance among them.

3. Balance Efficiency Analysis

The principle of balance efficiency to describe the operation of a solar cell is considered that the sun a Blackbody has a surface temperature of 6000 K. The generalization of Planck's radiation law for Blackbody and luminescent radiation is:

$$S_R = \frac{2\pi hc^2}{\lambda^5} \frac{1}{e^{((hc/\lambda - \mu)/kT)} - 1} \quad (1)$$

where S_R is solar spectrum, λ is wavelength of light, h is Planck's constant, c is the light speed, μ is the chemical potential, k is Boltzmann's constant, and T is the temperature of the Blackbody. From the Roosbroeck-Shockley equation, the flux of photons (φ) absorbed by the semiconductor or emitted from the semiconductor is [17]:

$$\varphi(\lambda_a, \lambda_b, T, \mu) = \int_{\lambda_a}^{\lambda_b} S_R \, d\lambda \quad (2)$$

Whereλ_a and λ_b are the lower and upper light wavelength at the energy limits of the photo flux for the corresponding transitions, respectively. When treating the sun as an ideal Blackbody and the solar absorption of a semiconductor is limited by the bandgap energy (E_g), the flux of photons absorbed at the sun's surface (φ_s) is:

$$\varphi_s(\lambda_a, \lambda_g, T_s, 0) = \int_{\lambda_a=0}^{\lambda_g} \frac{2\pi hc^2}{\lambda^5} \frac{1}{e^{(hc/\lambda kT_s)} - 1} d\lambda \quad (3)$$

Where λ_g is the light wavelength at the bandgap energy of the solar semiconductor, T_s is the temperature of the sun. The photon flux absorbed by the solar cell φ_{ssc} is:

$$\varphi_{ssc} = \varphi_s \times f_s \quad (4)$$

Where $f_s = 2.1646 \times 10^{-5}$ is called geometric parameter [14].

Similarly, the solar cell may be considered as an ideal Blackbody at temperature T_c = 300 K. Therefore, a photon emission from solar cell with a flux φ_{sc} is emitted when an electron-hole pairs is direct recombined.

$$\varphi_{sc}(\lambda_a, \lambda_g, T_c, 0) = \int_{\lambda_a=0}^{\lambda_g} \frac{2\pi hc^2}{\lambda^5} \frac{1}{e^{((hc/\lambda kT_c)-1}} d\lambda \quad (5)$$

According to the Shockley-Queisser model, the current density, *j*, of the solar cell device can be written as [31]:

$$j = q[c_s f_s \varphi_s(0, \lambda_g, T_s, 0) + (1 - c_s f_s)\varphi_{sc}(0, \lambda_g, T_c, 0) - \varphi_{sc}(0, \lambda_g, T_c, \mu)] \quad (6)$$

Wherec_s is the light intensity on a solar cell, it is called the number of suns, i.e., $c_s = 1$ at the surface of the Earth's atmosphere and $c_s = 1/f_s$ at the surface of the sun's. The chemical potential of luminescent photons , μ, is equal to the applied bias, *qV*, which it is equal to the amount of splitting in the quasi-Fermi energy levels. This equation represents the balance formula; it gives directly the current-voltage characteristics of a solar cell and the solar power conversion efficiency can be directly calculated.

4. Conventional Solar Cell

To illustrate the tradeoffs in material selection for CSC, the balance performance I-V characteristics of some elemental (Ge and Si) and binary (GaAs, AlSb, and GaP) semiconductors are shown in Fig. (2). This Figure illustrates the main problem of the CSCs which is when the output current increases the output voltage decreases and vice versa. Therefore, the optimum solar cell bandgap energy matches the maximum efficiency can be calculated from maximum solar cell output power which it is clearly shown in P-V characteristic, Fig. (3).

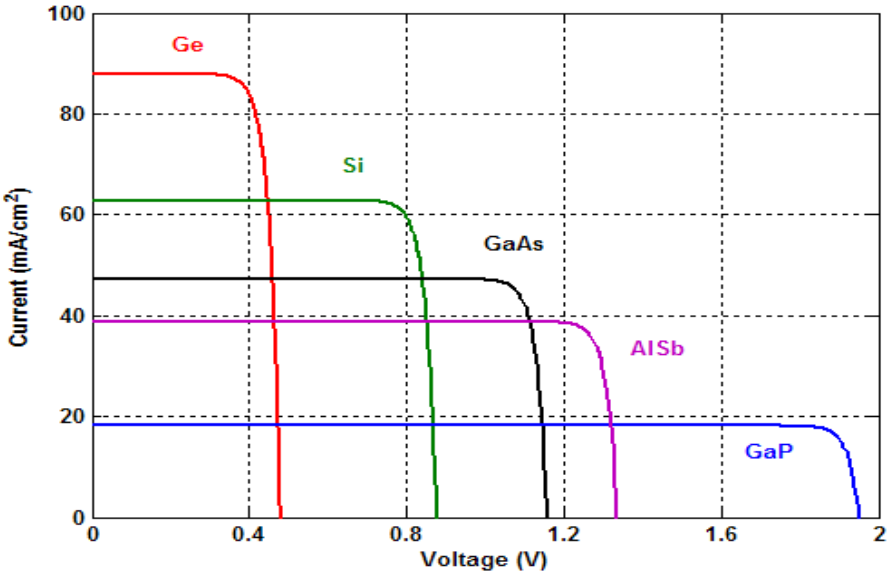

Fig. (2). I-V characteristics of some semiconductors solar cell

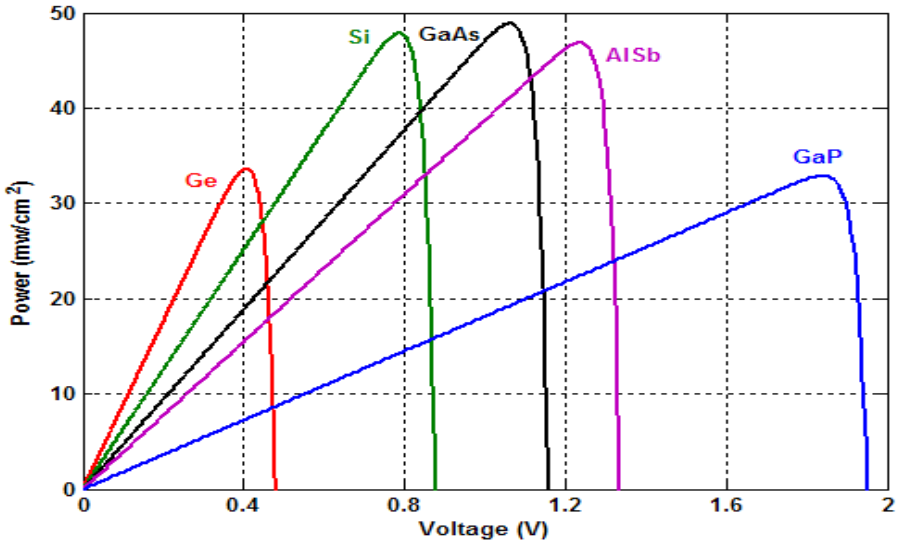

Fig. (3). P-V characteristics of some semiconductors solar cell

To determine the optimum bandgap energy of the CSC corresponding to the maximum efficiency, the solar cell efficiencies are analyzed with changing the bandgap energies at the Blackbody, AM0, and AM1.5 solar spectra and several different solar concentrations. The Blackbody, AM0, and AM1.5 spectra are plotted in Fig. (4). The Blackbody spectrum is calculated and used in theoretical analysis. The AM0 and AM1.5 spectra are measured by the American Society for Testing and Materials (ASTM) and represent the solar spectra at outside the Earth's atmosphere and at the surface of the Earth's respectively [32].

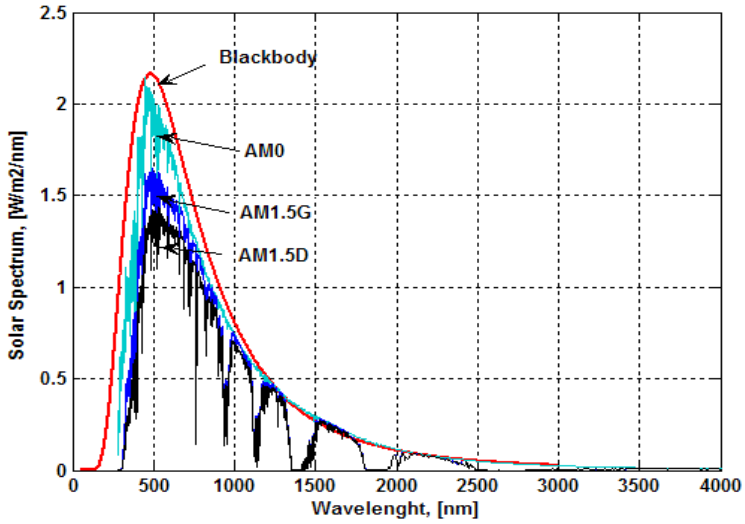

Fig. (4). Solar spectrum of Blackbody at 6000 K and more realistic solar spectra

Figure (5) illustrates this study, which it shows the balance efficiency with different material bandgap energies under Blackbody spectrum and more realistic AM0 and AM1.5 solar spectra. The effect of Blackbody and AM0 is approximately similar although the AM0 spectrum is not a smooth function. The AM1.5 is significantly different than the Blackbody and AM0 by presence the irregularity of the AM1.5 spectrum. The improve efficiencies for the AM1.5 are due to smaller value of the solar constants corresponding to this spectrum [14]. Table (1) summarizes the maximum efficiencies and optimum bandgap energies at 1 sun and maximum solar concentration for the three standard spectra. These data are plotted over the entire concentration range in Fig. (6). It is clear that the optimum design under one spectrum is not under another spectrum.

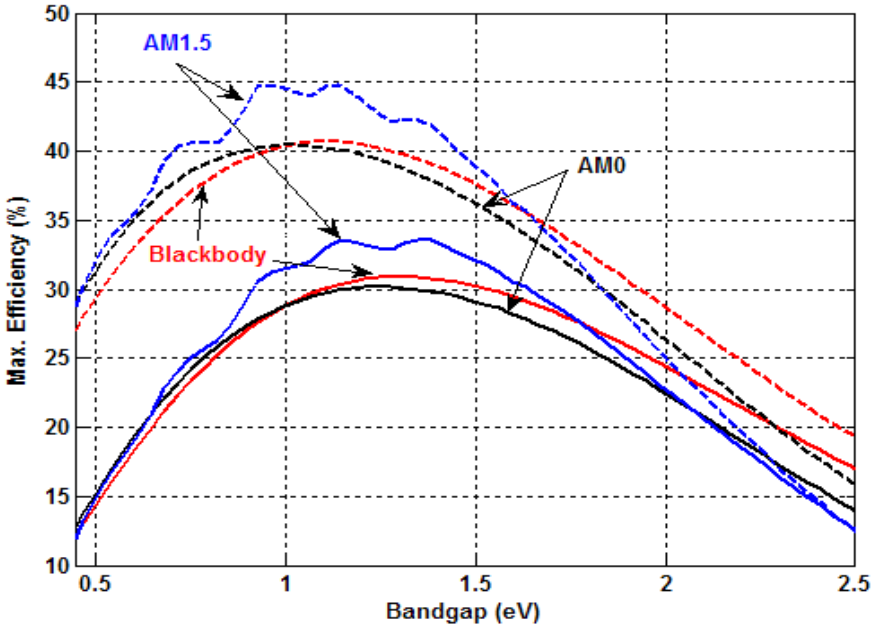

Fig. (5). Comparison of the maximum efficiencies of CSC for different bandgap energies and spectra at 1 sun (sold lines) and maximum solar concentration (dashed lines)

Table (1). Summarizes the maximum efficiencies and optimum bandgap energies at 1 sun and maximum concentration for the three standard spectra

Solar Spectra	1 Sun Concentration		Max. Concentration	
	Max. Efficiency (%)	Opt. Bandgap (eV)	Max. Efficiency (%)	Opt. Bandgap (eV)
Blackbody	30.93	1.31	40.71	1.10
AM0	30.17	1.28	40.43	1.00
AM1.5	33.58	1.35	44.83	0.96

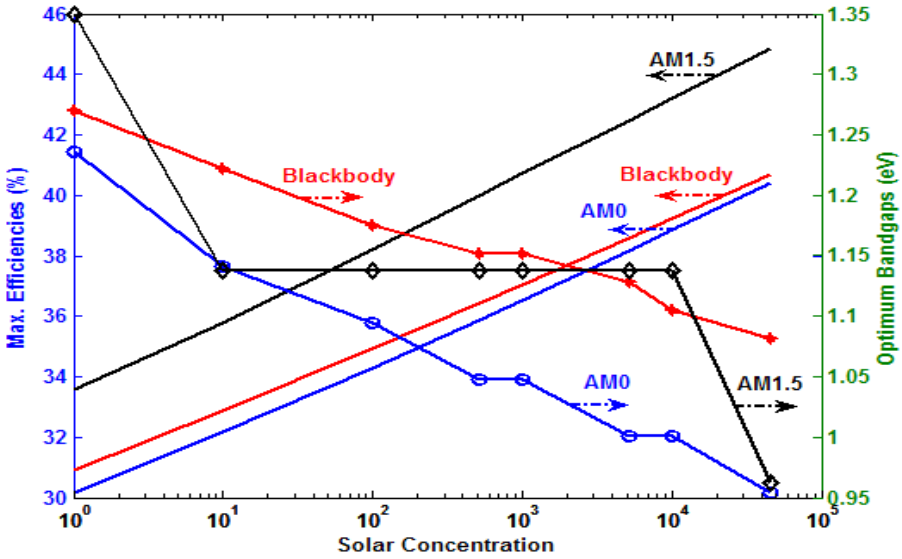

Fig. (6). Comparison between the three standard spectra with maximum efficiencies and optimum bandgap energies for CSC.

5. Intermediate Band Solar Cell

The conventional solar cell would only be able to absorb photons with energy equal to or greater than the energy between CB and valence band (VB), E_{CV}. For the nanostructure solar cell, a new band is located at an intermediate band level, E_I, between CB and VB. This band increases the absorb photons which leads to the increased performance of this design when compared to the CSC. To study a balance analysis of this type, the following assumptions are necessary [3, 10, 33]: (1)There is no overlap of energy transitions for a given photon energy, i.e., if a photon may energetically induce a transition from one band to another then all photons of the same energy will only cause that specific transition. (2) Electrons enter the IB only pumped from the VB and they leave only to the CB. (3) The difference in chemical potentials between any two bands is simply the difference between the quasi-Fermi levels of these bands.

According to these assumptions, the IBSC have three transitions of electrons between bands. The standard effect of an electronic transition across the bandgap energy, E_{CV}, gives j_{CV} as in previous analysis in section 4. The effect of the IB to CB transition, E_{CI}, produces j_{CI} which it must be equal to j_{IV} which it produces from the transition between the VB and IB, E_{IV}, according to the above assumptions. The two intermediate band transitions E_{CI} and E_{IV} are independent of each other whoever the conventional bandgap energy E_{CV} is a function of these bands. Therefore, the three generated currents are:

$$j_{CV} = q[c_s f_s \varphi_s(0, \lambda_{CV}, T_s, 0) + (1 - c_s f_s)\varphi_{sc}(0, \lambda_{CV}, T_c, 0) - \varphi_{sc}(0, \lambda_{CV}, T_c, \mu)]$$
$$j_{CI} = q[c_s f_s \varphi_s(\lambda_{CI}, \lambda_{IV}, T_s, 0) + (1 - c_s f_s)\varphi_{sc}(\lambda_{CI}, \lambda_{IV}, T_c, 0) - \varphi_{sc}(\lambda_{CI}, \lambda_{IV}, T_c, \mu_{CI})] \quad (7)$$
$$j_{IV} = q[c_s f_s \varphi_s(\lambda_{IV}, \lambda_{CV}, T_s, 0) + (1 - c_s f_s)\varphi_{sc}(\lambda_{IV}, \lambda_{CV}, T_c, 0) - \varphi_{sc}(\lambda_{IV}, \lambda_{CV}, T_c, \mu_{IV})]$$

Since the currents j_{CI} and j_{IV} must be equal, therefore the total current $j_T = j_{CV} + j_{CI}$. As in previous analysis, the chemical potential of photons is equal to the applied bias, $\mu = \mu_{CI} + \mu_{IV} = qV$, which it is equal to the amount of splitting in the quasi-Fermi energy levels. By following the same methodology in CSC, the balance efficiency is analyzed under different solar spectra at 1 sun and maximum solar concentration, and changing the IB location to give the maximum efficiency. Figures (7 - 9) and Table (2) show the balance efficiency, optimum bandgap energies, and the location of IB of IBSC at 1 sun and maximum solar concentration for the three standard spectra.

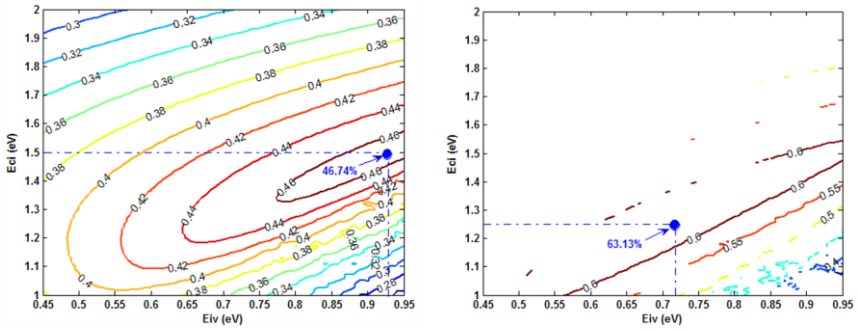

(a) **(b)**

Fig. (7). Balance efficiency of IBSC as it varies with the position of IB between the CB and VB at Blackbody spectrum under: (a) 1 sun, (b) Maximum solar concentration

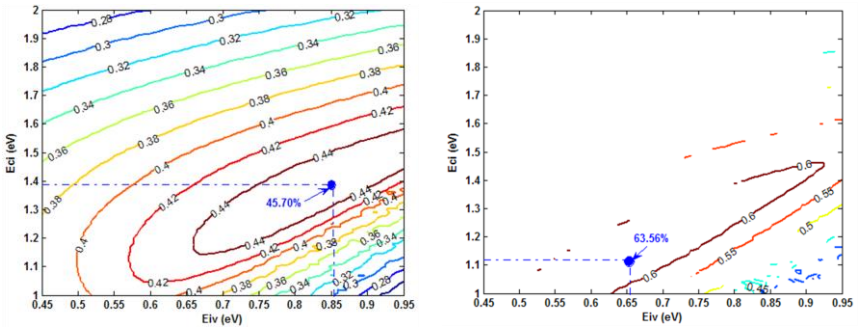

(a) **(b)**

Fig. (8). Balance efficiency of IBSC as it varies with the position of IB between the CB and VB at AM0 spectrum under: (a) 1 sun, (b) Maximum solar concentration

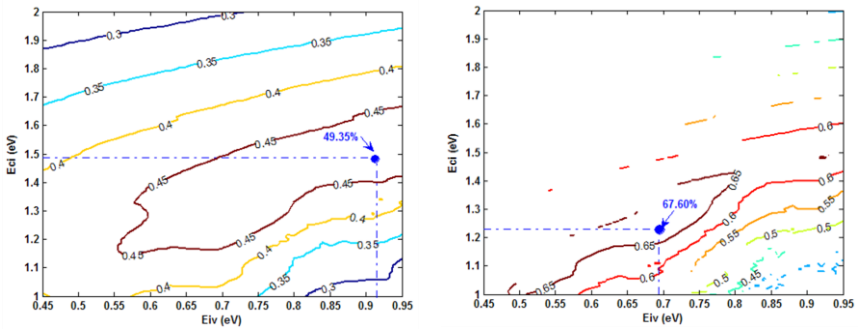

(a) **(b)**

Fig. (9). Balance efficiency of IBSC as it varies with the position of IB between the CB and VB at AM1.5 spectrum under: (a) 1 sun, (b) Maximum solar concentration

Table (2). Summarizes the maximum efficiencies and optimum bandgap energies and IB of IBSC at 1 sun and maximum solar concentration for the three standard spectra

Solar Spectra	1 Sun Concentration				Max. Concentration			
	Max. Efficiency (%)	Opt. Bandgap (eV)			Max. Efficiency (%)	Opt. Bandgap (eV)		
		E_{CI}	E_{IV}	E_{CV}		E_{CI}	E_{IV}	E_{CV}
Blackbody	46.74	1.50	0.93	2.43	63.13	1.25	0.72	1.97
AM0	45.70	1.39	0.86	2.25	63.56	1.12	0.66	1.78
AM1.5	49.35	1.49	0.93	2.42	67.60	1.23	0.69	1.92

Figure (7a) shows the balance efficiency under Blackbody spectrum at 1 sun as the maximum efficiency is 46.74% which it corresponds to IBs of E_{IV} = 0.93 eV and E_{CI} = 1.5 eV; the total bandgap energy E_{CV} = 2.43 eV. When the solar concentration is increased to its maximum value as shown in Fig.(7b), the efficiency is increased to 63.13% and the optimum values of both E_{IV} and E_{CI} decrease to 0.72 eV and 1.25 eV respectively. Also, the total bandgap energy is decreased to 1.97 eV. The efficiency of the IBSC does not depend on the order of the energy bands E_{CI} and E_{IV}. Efficiency depends only on the energy transition themselves. For example, the theoretical efficiency is equal to 63.13% under maximum solar concentration when E_{CI} = 1.25 eV and E_{IV} = 0.72 eV. However, the same result is also achieved when E_{CI} = 0.72 eV and E_{IV} = 1.25 eV, therefore the order of the energy transition is unimportant. Comparing the behavior of IBSC with Fig.(6) and Table (1) for the CSC, note that both of them demonstrate the same behavior where as the concentration of solar increases the efficiency increases and the large bandgap energy decreases. Also, it is clear that for the maximum solar concentration, the matching between j_{CI} and J_{IV} is difficult to obtain, it explains the absence of more possibilities for efficiency in Fig. (7b). Therefore, the location of IB is limited for maximum solar concentration.

Similar for CSC, the balance efficiency of the IBSC is more realistic when analyzed with the actual AM0 and AM1.5 solar spectra. The results are shown in Figs. (8) and (9). From Fig.(8), it is clear that the balance efficiency is similar due to the similarity between the Blackbody and AM0 spectra. Some aliasing is seen in the AM0 contours due to the irregularity of the AM0 spectrum. Also for AM1.5 in Fig.(9), the contours of the efficiencies are a much more irregular when compared with the Blackbody and AM0 analysis. Due to the large of irregularity in the AM1.5 spectrum, the several local maxima are present and thus the efficiency is increased.

The summary of the above discussion are plotted over the entire solar concentration range in Fig. (10). It is clear that the optimum design under one spectrum is not under another spectrum as in the CSC approximately.

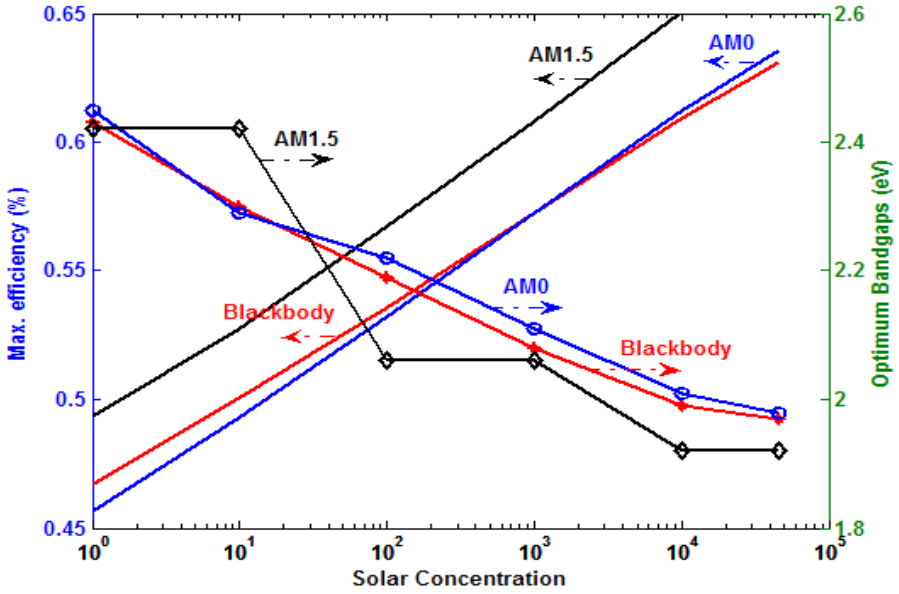

Fig. (10). Comparison between the three standard spectra with maximum efficiencies and optimum bandgap energies for IBSC

6. Quantum Dot Intermediate Band Solar Cell

For this type of solar cell, the size, shape, and spacing of the quantum dots in the barrier material are very important to improve the efficiency of the device. Whenever the quantum dots are arranged uniform in the barrier material, the IBs are well-placed and the recombination is reduced. Various techniques such as Metal Organic Chemical Vapor Deposition (MOCVP) and Molecular Beam Epitaxy (MBE) are available to produce highly uniform QD arrays in barrier material [13, 34]. In this paper, we assume that the geometry of the QD is cubic and therefore it is characterized by one dimension. Also, to simplify the analysis, we assume that no valance band offset (VBO) and the only confining potential occurs at the conduction band offset (CBO). Under these assumptions, the time-independent Schrödinger Equation and the Krong-Penny model are used to calculate the energy bands in the QDs using the effective mass of charge carriers [8, 34]. In this work, $Al_{1-x}Ga_xAs/In_{1-y}Ga_yAs$ QDIBSC is analyzed theoretically. Where $Al_{1-x}Ga_xAs$ is the barrier ternary alloy and $In_{1-y}Ga_yAs$ is the QD ternary alloy. The bandgap energies, E_g, and effective masses of these alloys, m^*, are calculated by the following chemical formulas [5, 35]:

For barrier ternary alloy material

$$E_{g(Al_{1-x}Ga_xAs)} = 3.099(1-x) + 1.519x - 0.2x(1-x),$$
$$m^*_{(Al_{1-x}Ga_xAs)} = (1-x)m^*_{(AlAs)} + xm^*_{(GaAs)}$$

For QD ternary alloy material

$$E_{g(In_yGa_{1-y}As)} = 1.519(1-y) + 0.417y - 0.588y(1-y),$$
$$m^*_{(In_yGa_{1-y}As)} = (1-y)m^*_{(GaAs)} + ym^*_{(InAs)}$$

Where ***x*** and ***y*** are limited between 0 and 1. They are called the molar concentration for GaAs and InAs in barrier and QD ternary alloys materials, respectively.

The compound semiconductors which are used in this study for QDIBSC are $Al_{0.4}Ga_{0.6}As/In_{0.42}Ga_{0.58}As$ [36, 37]. The bandgap of ternary alloy $In_{0.42}Ga_{0.58}As$ (0.913 eV) dot array material is smaller than the bandgap of ternary alloy $Al_{0.4}Ga_{0.6}As$ (2.103 eV) barrier or bulk material to induce the IB by coupling of confined electronic states in the $In_{0.42}Ga_{0.58}As$ conduction band. The bandgap energies of the structure of $Al_{0.4}Ga_{0.6}As/In_{0.42}Ga_{0.58}As$ QDIBSC are approximately close to the ideal values determined from Table (2) in the pervious section. The balance efficiency for this structure under the above assumptions is plotted in Figs (11 - 13) and summarized in Table (3). From the first point of view when comparing the Figs (11 - 13) and Table (3) with the results in Figs (7 - 9) and Table (2), it is clear that the proposed model is approximately ideal because it is based on the difficult of technology for ternary semiconductor materials.

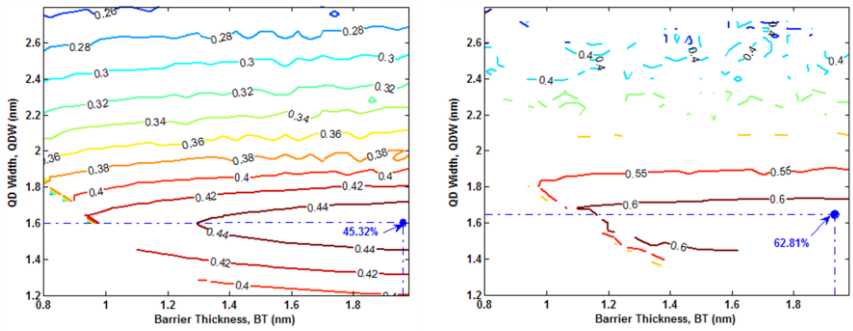

(a) **(b)**

Fig. (11). Balance efficiency of QDIBSC as it varies with the BT and QDW at Blackbody spectrum under: (a) 1 sun, (b) Maximum sola concentration

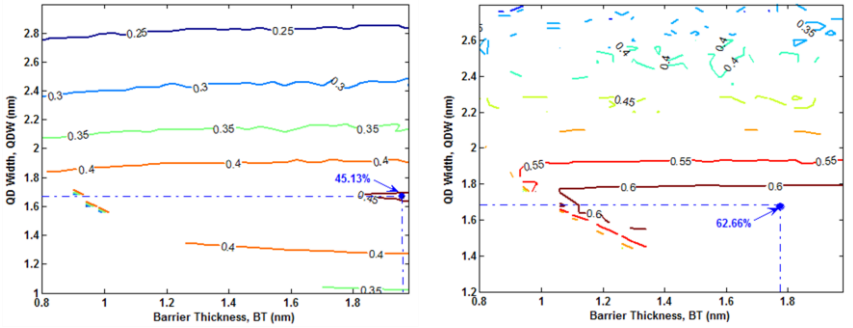

(a) **(b)**

Fig. (12). Balance efficiency of QDIBSC as it varies with the BT and QDW at AM0 spectrum under: (a) 1 sun, (b) Maximum solar concentration

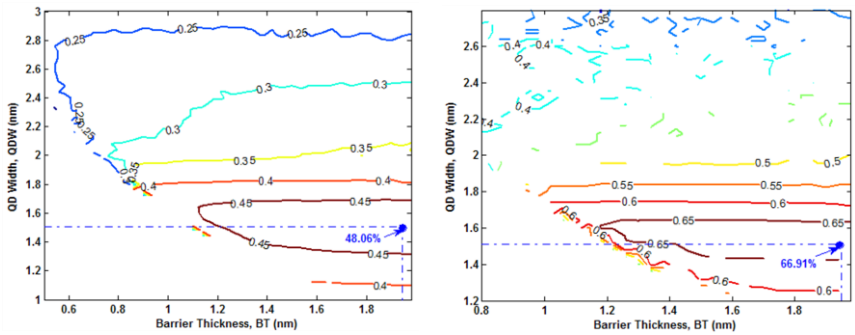

(a) **(b)**

Fig. (13). Balance efficiency of QDIBSC as it varies with the BT and QDW at AM1.5 spectrum under: (a) 1 sun, (b) Maximum solar concentration

Table (3). Summarizes the maximum efficiencies and optimum BT and QDW of QDIBSC at 1 sun and maximum solar concentration for the three standard spectra

Solar Spectra	1 Sun Concentration				Max. Concentration			
	Max. Efficiency (%)	Opt. Barrier thickness, BT & QD width, QDW (nm)		IB Width (eV)	Max. Efficiency (%)	Opt. Barrier thickness, BT & QD width, QDW (nm)		IB Width (eV)
		BT	QDW			BT	QDW	
Blackbody	45.32	1.98	1.60	0.0696	62.81	1.94	1.64	0.0684
AM0	45.13	1.98	1.68	0.0612	62.66	1.78	1.68	0.0756
AM1.5	48.06	1.98	1.52	0.0792	66.91	1.98	1.52	0.0792

The results in Figs (11 - 13) show the effect of QDW and BT in the efficiency of QDIBSC at 1 sun and maximum solar concentration under different spectra. Before discuss the results in Figs (11 – 13), Fig (14) shows changing of the first energy bandwidth of IB when changing the BT and QDW. It is clear that the larger width of QDs and BT tend to decrease the first energy bandwidth of the IB and it moves toward the VB therefore E_{ci} increases and E_{iv} decreases.

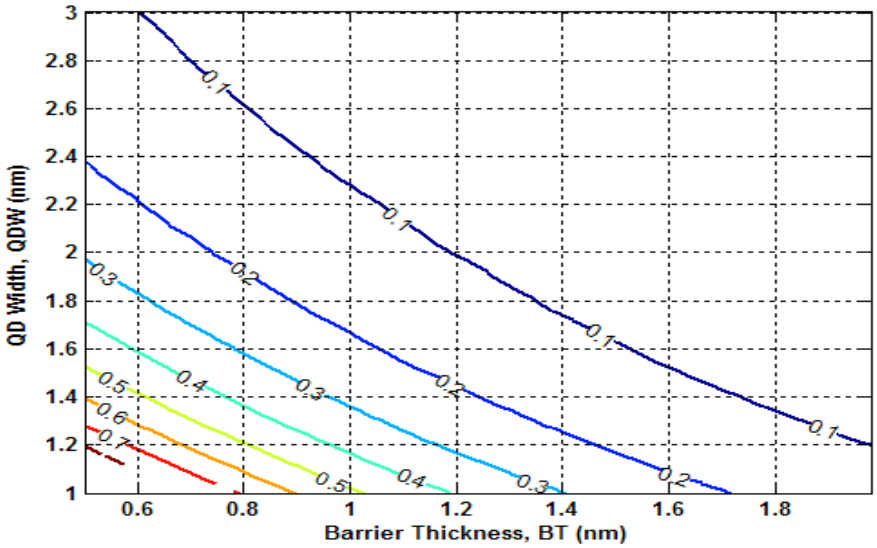

Fig. (14). Width of IB energy (eV) when changing BT and QDW (nm)

This work studied QDIBSC with only one IB therefore the QDW and BT in this type of ternary materials are limited with the values in Fig. (14), i.e., 1 nm ≤ QDW ≤ 3 nm and 0.5 nm ≤ BT ≤ 2 nm. From the results in Figs (11 – 13), the maximum energy conversion efficiency of $Al_{0.4}Ga_{0.6}As/In_{0.42}Ga_{0.58}As$ QDIBSC as a function of QDW and BT under different solar spectra is changed from 45.32% to 48.06% at 1 sun, and from 62.66% to 66.91% at the maximum solar concentration. These curves illustrate that the efficiency of this structure is not available for all limits of QDW and BT that are mentioned above. When the QDW decreases toward low limit; the BT increases to upper limit. Another note for these curves is that the overall QDIBSC realizes current-matching easily for 1 sun than the maximum solar concentration which it is very difficult. Table (3) summarizes the maximum efficiencies and optimum BT and QDW of QDIBSC at 1 sun and maximum solar concentration for the three standard spectra.

7. Conclusions and Future Works

In this paper, the balance efficiency of conventional and nanostructure solar cell dependent on Shockley and Queisser model has been studied under more realistic solar spectra, in addition to the standard Blackbody spectrum. For the nanostructure or QDIBSC, the balance analysis showed that it varies with the location of the intermediate band within the bulk semiconductor bandgap energy. Therefore, the optimum location of intermediate band which gives the maximum energy conversion efficiency can be determined. Accordingly, the choice of materials for

solar cell implementation to achieve these results is easy. In this work, the parameters of QDIBSC structure have been determined based on the balance efficiency by using the Schrödinger Equation and the Krong-penny model. The results have shown that both the location of the IB and the energy conversion efficiency strongly depend on the width of the QD and the barrier thickness. The maximum efficiency is changed from 62.66% to 66.91% under the maximum solar concentration at different solar spectra for only one IB of $Al_{0.4}Ga_{0.6}As/In_{0.42}Ga_{0.58}As$ QDIBSC, although it is very difficult to obtain the current-matching in the QDIBSC.

In future works, additional energy levels in QDIBSC to increase the efficiency will consider and when searching for the optimally energy bands placed must take into account the bands overlaps with each other or with the CB and VB. This condition is necessary because the bandgap of the barrier material is reduced therefore the operating voltage and output power of the cell's are decreased. Also, the searching for new and more promising materials with significant sub-bandgap absorption, high mobility, and suppressed non-radiative processes is crucial for the success of intermediate band devices. This might include alloys and quantum confined structures. The theoretical and modeling effort should focus on explanation of the low efficiencies observed in real devices, revealing the underlying physical reasons, and provides feasible solutions to the problems. In addition, continued effort on theoretical work can predict/propose novel concepts to either exceed current efficiency limits or more practically.

8. References

[1] **Sablon, K., Little, J., Mitin, V., Sergeev, A., Vagidov, N. and Reinhardt, K.,** "Strong Enhancement of Solar Cell Efficiency Due to Quantum Dots with Built-In Charge", *NanoLett.*, 11, (2011), pp. 2311-2317.

[2] **Tanabe, K., Guimard, D., Bordel, D., Morihara, R., Nishioka, M. and Arakawa, Y.,** "High-Efficiency InAs/GaAs Quantum Dot Solar Cells by MOCVD", *38th Photovoltaic Specialists Conference (PVSC)*, Austin, Texas, (2012), pp. 1929 – 1930.

[3] **Lin, C., Liu, W. and Yu Shih, C.,** "Detailed balance model for intermediate band solar cells with photon conservation", *International online journal of Optics*, Vol. 19, Issue 18, (2011), pp. 16927 – 16933.

[4] **Bremner, S. P., Pancholi, A., Ghosh, K., Dahal, S., Liu, G. M., Ban, K. Y., Levy, M. Y. and Honsberg, C. B.,** "Growth of InAs Quantum Dots on GaAsSb for the Realization of a Quantum Dot Solar Cell", *33rd **Photovoltaic Specialists Conference (PVSC),*** San Diego, CA, USA, (2008), pp. 1– 6.

[5] **Qing-Wen, D., Xiao-Liang, W., Cui-Bai, Y., Hong-Ling, X., Cui-Mei, W., Hai-Bo, Y., Qi-Feng, H., Yang, B., Jin-Min, L., Zhan-Guo, W. and Xun, H.,** "Computational Investigation of $In_xGa_{1-x}N$/InN Quantum-Dot

Intermediate-Band Solar Cell", *Chinese Physics Letters*, Vol. 28, No. 1, (2011), pp.1-4.

[6] **Linares, P. G., Marti, A., Antolin, E., Ramiro, I., Lopez, E., Farmer, C. D., Stanley, C. R. and Luque, A.,** "Low-Temperature Concentrated Light Characterization Applied to Intermediate Band Solar Cells", *IEEE Journal of Photovoltaics*, Vol. 3, No. 2, (2013), pp. 753-761.

[7] **Farrell, D., Takeda, Y., Nishikawa, K., Nagashima, T., Motohiro, T., Ekins-Daukes, N. and Okada, Y.,** "A New Type of Hot-carrier Solar Cell Utilizing Thermal Up and Down Conversion of Sunlight", *Appl. Phys. Lett.*, 111102, (2011), pp. 99.

[8] **Xiaosheng, Q., Sisi, Z., Hongyin, B. and Liling, X.,** "The effect of InAs quantum-dot size and inter-dot distance on GaInP/GaAs/GaInAs/Ge multi-junction tandem solar cells", *Journal of semiconductor*, Vol. 34, No. 6, (2013), pp. 062003-1 – 062003-5.

[9] **Chukwuocha, E. O. and Onyeaju, M. C.,** "Effect of Quantum Confinement on the Wavelength of CdSe, ZnSandGaAs Quantum Dots (QDs)", *International Journal of Scientific & Technology Research*, Vol. 1, Issue 7, (2012), pp. 21 -24.

[10] **Antolin, E., Marti, A. and Luque, A.,** "The Lead Salt Quantum Dot Intermediate Band Solar Cell", *37th Photovoltaic Specialists Conference (PVSC)*, Seattle, WA, USA, (2011), pp. 1907-1912.

[11] **Kosyachenko, L.,** *Solar Cells – New Aspects and Solutions*, InTech, Open access book, ISBN 978-953-307-761-1, (2011).

[12] **Ogura, A., Morioka, T., Garcia, P., Hernandez, E., Ramiro, I., Antolin, E., Marti, A., Luque, A., Yamaguchi, M. and Okada, Y.,** "Modeling of Quantum Dot Solar Cells for Concentrator PV Applications", *37th Photovoltaic Specialists Conference (PVSC)*, Seattle, WA, USA, (2011), pp. 2642 – 2645.

[13] **Ojajarvi, J.,** *Tetrahedral chalcopyrite quantum dots in solar-cell applications*, Msc. Thesis, Jyvaskyla University, Finland, (2010).

[14] **Steven, E. J.,** *Quantum Dot Intermediate Band Solar Cells: Design Criteria and Optimal Materials*, PhD Thesis, Drexel University, Philadelphia, Pennsylvania, USA, (2012).

[15] **Anderson, N. G.,** "On quantum well solar cell efficiencies", *Physica E*, 14, (2002), pp. 126– 131.

[16] **Luque, A. and Marti, A.,** "Thermodynamic consistency of sub-bandgap absorbing solar cell proposals", *IEEE Transactions on Electron Devices*, 49, (2001), pp. 2118 – 2124.

[17] **Van Roosbroeck, W., Shockley, W.,** "Photon-Radiative Recombination of Electrons and Holes in Germanium", *Phys. Rev. 94*, (1954), pp. 1558-1560.

[18] **Marti, A., Cuandra, L. and Luque, A.,** "Quantum dot intermediate band solar cell", *28th IEEE PVSC*, Anchorage, Alaska, (2000), pp. 940 – 943.

[19] **Schokley and Queisser,** "Detailed balance limit of efficiency of p-n junction solar cell", *J. Appl. Phys.*, vol. 32, (1961), pp. 510-519.

[20] **Green, M. A., Emery, K., Hishikawa, Y. and Warta, W.,** "Solar Cell Efficiency Tables (Version 32)", *Prog. Photovolt. Res. Appl.*, vol. 16, issue 5, (2008), pp. 435-440.

[21] **Linge, C.,** *Modeling of the Intermediate Band Tandem Solar Cell Using the AM1.5 Spectra*, MSc. Thesis, Department of Physics, University of Science and Technology, Norwegian, (2011).

[22] **Luque A. and Martı, A.,** "Increasing the Efficiency of Ideal Solar Cells by Photon Induced Transitions at Intermediate Levels", *Phys. Rev. Lett.*, vol. 78, (1997), pp. 5014.

[23] **Cress, C. D., Hubbard, S. M., Landi, B. J., Raffaellea, R. P. and Wilt, D. M.,** "Quantum dot solar cell tolerance to alpha-particle irradiation", *Appl. Phys. Lett.*, vol. 91, (2007), pp. 183108.

[24] **Luque, A.,** "Operation of the intermediate band solar cell under nonideal space charge region conditions and half filling of the intermediate band", *J. Appl. Phys.*, vol. 99, (2006), pp. 094503 – 094503-9.

[25] **Aly, A. M. and Nasr, A.,** "Theoretical Performance of Solar Cell based on Mini-bands Quantum Dots", *J. Appl. Phys.*, Volume 115, Issue 114311, (2014), pp. 114311 – 114311-9.

[26] **Aly, A. M. and Nasr, A.,** "Theoretical Study of One-Intermediate Band Quantum Dots Solar Cell", *International Journal of Photoenergy*, Volume 2014, Article ID 904104, (2014), pp. 1-10.

[27] **Aly, A. M.,** "Progress into power conversion efficiency for solar cells based on nanostructured and realistic spectra", *Journal of Renewable Sustainable Energy*, Volume 6, Issue 023118, (2014), pp. 023118 – 023118-9.

[28] **Schmeits, M. and Mani, A. A.,** "Impurity photovoltaic effect in c –Si solar cells. A numerical study", *J. Appl. Phys.*, vol. 85, (1999), pp. 2207-2212.

[29] **Walukiewicz, W. and Yu, K. M.,** *Ultrahigh Efficiency Multiband Solar Cells Final Report for Director's Innovation Initiative Project*, Lawrence Berkeley National Laboratory LBNL Report 59768, (2006).

[30] **Kurtz, S., Johnston, S. W., Geisz, J. F., Friedman, D. J. and Ptak, A. J.,** *Effect of Nitrogen Concentration on the Performance of* $Ga_{1-x}In_xN_yAs_{1-y}$

Solar Cells, National Renewable Energy Laboratory, Golden, Colorado NREL/CP-520-37361, (2005).

[31] **Shockley W. and Queisser, H. J.,** "Detailed balance limit of efficiency of *p-n* junction solar cells", *J. Appl. Phys. 32*, (1961), pp. 510-519.

[32] **Linge, C.** *Modeling of the Intermediate Band Tandem Solar Cell Using the AM1.5 Spectra*, MSc. Thesis, Department of Physics, University of Science and Technology, Norwegian, (2011).

[33] **Kurome, A., Morigaki, R. Souma, S. and Ogawa, M.,** "Analysis of Electronic Structure in Quantum Dot Arrays for Intermediate Band Solar Cells", *IMFEDK*, Kansai, (2011), pp. 114-115.

[34] **Aguinaldo, R.** *Modeling Solutions and Simulations for Advanced III-V Photovoltaics Based on Nanostructures*, M.Sc thesis in Materials Science & Engineering, College of Science, Rochester Institute of Technology, Rochester, NY, (2008).

[35] **Ferhat, M.,** "Computational Optical bandgap Bowing of III-V Semiconductors Alloys", *Phys. Stat. Sol.*, Vol. 241, No. 10, (2004), pp. 38-41.

[36] **Popescu, V., Bester, G., Hanna, M., Norman, A. and Zunger, A.,** "Theoretical and experimental examination of the intermediate-band concept for strain-balanced (In,Ga)As/Ga(As,P) quantum dot solar cells", *Physical review B 78*, (2008), pp. 205321- 205321-17.

[37] **Kechiantz, A., Afanasev, A. and Lazzan, J.**, "Modification of band alignment at interface of $Al_yGa_{1-y}Sb/Al_xGa_{1-x}As$ type-II quantum dots by concentrated sunlight in intermediate band solar cells with separated absorption and depletion regions", *SPIE Photonics West*, San Francisco, CA, USA, (2013), pp. 1-6.

تحسين كفاءة تحويل الطاقة من الخلايا الشمسية

أبوالمعاطي متولي متولي علي [٢،١]

قسم الكترونيات الطاقة العالية وتحويل الطاقة، معهد بحوث الإلكترونيات،

مبنى المركز القومى للبحوث، جمهورية مصر العربية [١]

قسم هندسة الحاسب، كلية الحاسب، جامعة القصيم، بريدة، المملكة العربية السعودية [٢]

a_aly@qu.edu.sa & abouelmaaty67@gmail.com

(قدم للنشر في ٢٠١٤/٥/٢٧ م ، وقبل للنشر في ٢٠١٤/١٠/١٢ م)

ملخص البحث. في هذا البحث ابعاد النانو استخدمة لتحسين كفاءة تحويل الطاقة من الخلايا الشمسية. الكم النقطي لنطاق الطاقة الواسطي (QDIB)أُستخدم لهذا الغرض. هذه الفكرة تحافظ على القيمة العالية للجهد عندما لايوجد تيار يمر في الدائرة والتي تسمى (Open Circuit Voltage)مع زيادة التيار المتولد في الخلية الشمسية عند سقط ضوء الشمس عليها. سوف يتم تحليل كفاءة الخلايا الشمسية بستخدام طيف الجسم الاسود (Blackbody) وكذلك أطياف أكثر واقعية مثل AM0 و AM1.5. تم عمل مقارنة من ناحية الكفاءة بين الخلايا الشمسية التقليدية، الخلايا الشمسية ذات النطاق الطاقة الواسطي، الخلايا الشمسية ذات النطاق الطاقة الواسطي باستخدام الكم النقطي. أستخدمة معادلة شرودنجر لحساب نطاقات الطاقة الفرعية المستخدمة في نقل الطاقة وذلك عن طريق الكم النقطي وحجم الشحنات الناقلة للطاقة. كذلك تم دراسة تأثير كل من نطاقات الطاقة الفرعية المستخدمة في نقل الطاقة، مكان نطاق الطاقة الواسطي، حجم الكم النقطي، المسافة بين الكم النقطي على كفاءة تحويل الطاقة من الخلايا الشمسية. النتائج أوضحت أن كفاءة تحويل الطاقة من الخلايا الشمسية تحسنت بشكل ملحوظ عند استخدام الابعاد النانونية.